

---

# Modular Inverse Reinforcement Learning on Human Motion

---

**Shun Zhang**

Department of Computer Science  
University of Texas at Austin  
Austin, TX 78712  
menie482@cs.utexas.edu

**Matthew Tong**

Center for Perceptual Systems  
University of Texas at Austin  
Austin, TX 78712  
mhtong@gmail.com

**Mary Hayhoe**

Center for Perceptual Systems  
University of Texas at Austin  
Austin, TX 78712  
hayhoe@utexas.edu

**Dana Ballard**

Department of Computer Science  
University of Texas at Austin  
Austin, TX 78712  
dana@cs.utexas.edu

## Abstract

Reinforcement learning has been seen as a useful model for understanding human behavior because of the importance of the neural reward circuitry. However, because of the difficulty of scaling up RL models to large state spaces, it has been hard to apply these models to complex human behaviors. One potential simplification, consistent with observations of natural behavior, is that complex tasks can be broken down into independent sub-tasks, or modules. In this paper, we use observed human behavior while walking along a path to estimate the intrinsic reward values associated with different modular sub-tasks. To do this we use a simplified version of Inverse Reinforcement Learning to calculate the reward associated with path following, obstacle avoidance, and target collection of humans acting in an immersive virtual environment. Using the estimated values, a modular RL model can generate realistic behavior consistent with human action choices. This provides a way of understanding momentary sensorimotor decisions made in complex natural environments.

**Keywords:** Reinforcement learning, human motion, inverse learning

# 1 Introduction

A large body of evidence from human and other primate studies suggests that they use reinforcement signals to learn tasks and reinforcement learning has proved to be a good model for this process. However humans are able to learn and carry out very complex tasks involving many different objectives. How can they do this? The likelihood is that they use reinforcement in this context as well, but most formal reinforcement learning models do not scale well with increasing complexity.

One promising possibility is that the complex task can be broken down into sub-tasks that are each learned separately [6, 5, 1]. For certain task venues, this decomposition allows the behavior in the complex task to be chosen based on the value of a weighted sum of individual sub-task priorities. This paper explores the use of such a decomposition to characterize complex behavior of subjects in a virtual reality environment. The methodology of [5] allows the task priorities to be estimated using the subjects' behavioral data. Our experimental analysis shows that the modular reinforcement can be a surprisingly good model of behavior, predicting individual subjects' sub-task priorities in a way that explains their behavioral choices.

This paper is organized as follows. Section 2 introduces the domain and the composite task structure that we collected human data. Section 3 describes the main algorithm, modular inverse reinforcement learning. We report our experiment results in Section 4, and conclude in Section 5.

## 2 Multi-objective Domain

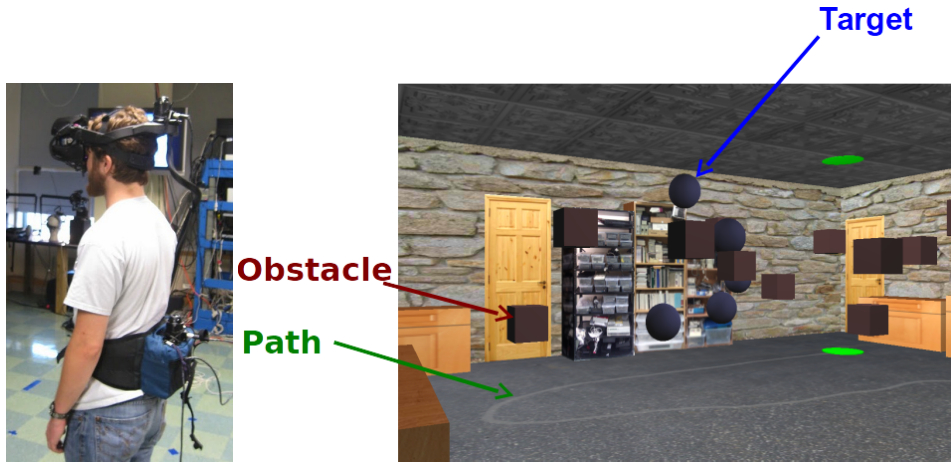


Figure 1: (Left) A human subject with a head mounted display (HMD) and trackers for the eye, head, and body. (Right) The environment the human can see through the HMD. The red cubes represent obstacles. The blue balls represent targets. There is also a gray path on the ground that the human subject can follow.

Figure 1 shows the experimental domain. The human subject was immersed in a virtual reality domain by wearing a binocular head-mounted display. The subject's eye, head, and body motion were tracked as he/she walked through a virtual environment that was designed to match the dimensions of a standard indoor environment. The subject was asked to follow the path, avoid the obstacles (red cubes), and collect the targets (blue spheres) by intercepting them. In different conditions they were asked to give different importance to particular sub-tasks, with sub-tasks being either relevant or irrelevant. Subjects were given auditory feedback when running into obstacles, and when intercepting targets, depending on their importance in the current condition. Thus this domain can be modeled by three modules, 1) following the path, 2) collecting targets, 3) avoiding obstacles. This general paradigm has been used to evaluate modular reinforcement learning [4, 5] and understand human behavior [9].

We evaluate four different tasks. **Task 1**, following the path only, and ignoring other objects. **Task 2**, following the path, while avoiding the obstacles. **Task 3**, following the path, while collecting targets. **Task 4**, following the path, collecting the targets and avoiding obstacles simultaneously. We conducted experiments using 4 human subjects who walked through the environment 8 times with different configurations of objects, in each of these 4 conditions. We asked whether an agent with modules trained for these three sub-tasks could generate paths that matched human's behavior.

### 3 Modular Inverse Reinforcement Learning

In Reinforcement Learning, when given a state and action pair,  $s$  and  $a$ , the function  $Q(s, a)$  evaluates the utility of taking action  $a$  from state  $s$ . The *policy* of a state is the action with the maximum Q value [8]. So how do we determine the global policy from the modules, or sub-tasks?

In the literature, modular formation is proposed for understanding human visuomotor behavior [7]. A combination of various basic modules can generate complex behavior to match human behavior. The combination can be either of Q functions of modules [5] or of rewards of modules [4]. Following [7, 5], we consider how the modules can be combined. Here we assume that the global Q function is a weighted sum of all  $Q_i$ , where  $Q_i$  is the Q function for i-th module.

$$Q(s, a) = \sum_i w_i Q_i(s_i, a)$$

where  $w_i$  is the weight of the i-th sub-MDP.  $w_i \geq 0, \sum_i w_i = 1$ .  $s_i$  denotes the decomposition of  $s$  in the i-th module.

Different weights can yield different performance. Let  $w$  be the vector of  $(w_1, w_2, w_3)$ , where  $w_1, w_2, w_3$  are weights for the sub-tasks of target et al collection, obstacle avoidance, and path following, respectively. An agent with  $w = (1, 0, 0)$  only collects targets, and one with  $w = (0, 0.5, 0.5)$  may avoid the obstacles and follow the path.

To obtain the weights given the samples of observed human behavior, we use inverse reinforcement learning. In reinforcement learning, we derive optimal policies given an MDP. In inverse reinforcement learning, however, aims to find out the underlying MDP by observing policies. A common way is to use a maximum likelihood method to recover the transition function and the reward function [3], but this approach is very expensive as some kind of learning is used in the innermost search loop. The modular approach allows a much more economical approach [5], since we module weights are the only free parameters. The transition function is known, and the reward function is trivially the weighted sum of that of modules. More precisely, we use the modular inverse reinforcement learning method in [5] to maximize the function below.

$$\max_w \prod_t \frac{e^{\eta Q(s^{(t)}, a^{(t)})}}{\sum_b e^{\eta Q(s^{(t)}, b)}} \quad (1)$$

where  $s^{(t)}$  is the state at time  $t$ , and  $a^{(t)}$  is the action at time  $t$ , which are both from samples.  $Q(s, a) = \sum_i w_i Q_i(s_i, a)$ , as defined before.  $\eta$  is a hyperparameter that determines the consistency of human's behavior. The larger  $\eta$  is, the algorithm is more likely to overfit the data.

The intuition of Equation 1 is that if an action is observed from the sample, then the Q value of taking that action should be larger compared to Q values of taking other actions.

### 4 Experiments

We trained the modules first to obtain  $Q_i$  before running the inverse reinforcement learning algorithm. For each module, the agent only considers the closest target and the closest obstacle. For the path module, the path was defined as segments connected by waypoints, so only the next waypoint is considered. The agent takes the distance and angle to the closest objects as the state representation. To make our weights represent the significance of the modules, we normalized the sub-MDPs with the unit (positive or negative) reward. The reward is 1 for collecting a target, -1 for running into an obstacle, and 1 for collecting a waypoint of the path. In the implementation, we made the radius of waypoints larger than that of other objects, so that the agent will not cling too much to the path.

We set some constraints on the learning agent in order to make it walk roughly like a human while keeping the action space small. We observed from the human trajectories that humans walk smoothly and do not turn sharply. Our agent was only allowed to do three actions — going straight ahead (0.3 meter), turning left with a small step (30 degrees to the left), and turning right with a small step (30 degrees to the right).

The results are shown in Figure 2. As in Figure 1, the red circles are obstacles and the blue circles are targets. The gray lines are the path. The black lines are trajectories of individual human subjects, with each line representing one human trajectory. Using the weights recovered by IRL, the trajectories of the agents are drawn in green. Although individual subjects varied in how they avoided obstacles or collected targets, the agent can figure out what the humans are doing on aggregate, and perform similarly. Figure 3 evaluates the performance by showing the number of targets hit and number of obstacles hit. The number of targets hit should be large, and the number of obstacles hit should be small, when the corresponding module is active. We can observe that humans still do better than the agent in these tasks. Nevertheless, the agent performance is quite similar to that of the human subjects.

In Figure 4, we show the log of values of Equation 1 for different weights. The white color represents higher probability. We can observe the centroids of white zones move for different tasks. It stays at the origin in Task 1, so neither the target

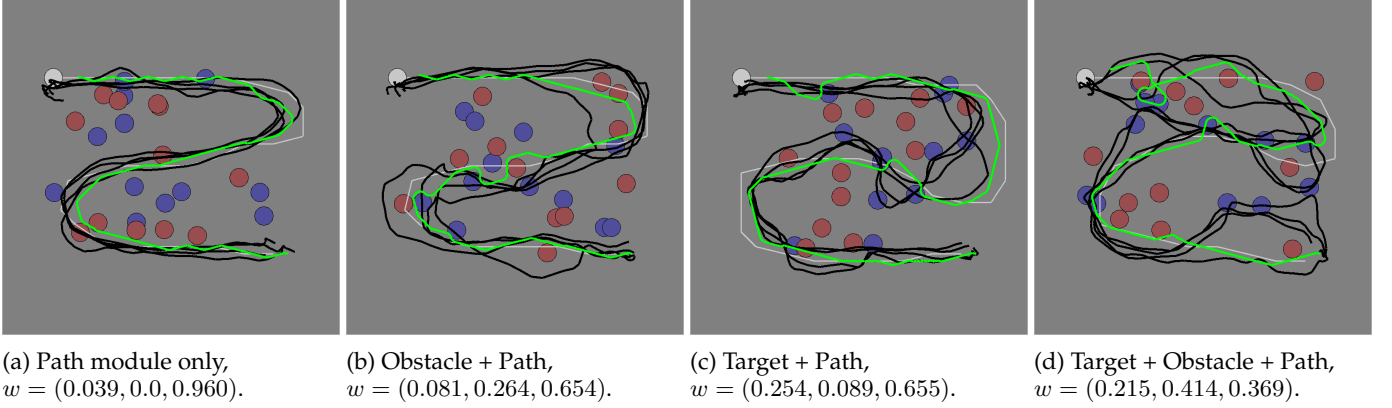


Figure 2: The trajectories of humans and the agent in the four tasks. Targets are blue and obstacles are red. The black lines are trajectories of human subjects, and the green lines are trajectories of the learning agent by using the optimum weights,  $w$ , derived from modular inverse reinforcement learning. Weights for each task are given as (target, obstacle, path).

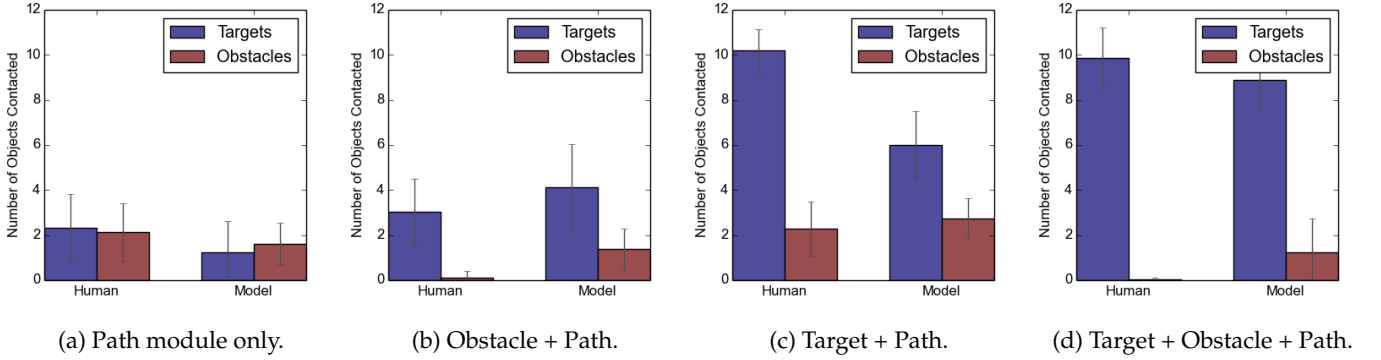


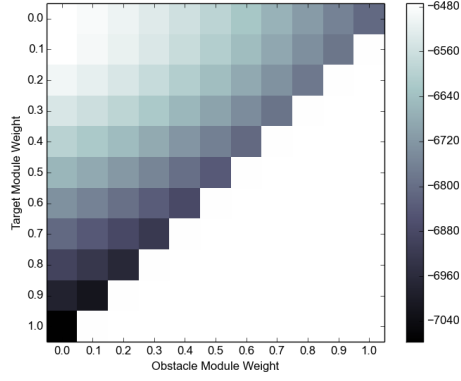
Figure 3: Number of targets hit and number of obstacles hit of the human subjects and the agent.

module nor the obstacle module is active. It moves away from the origin when a module is active. From the heatmaps, we find that fairly well-defined optima exist for these tasks. The optimal weights are also consistent with the experiment context.

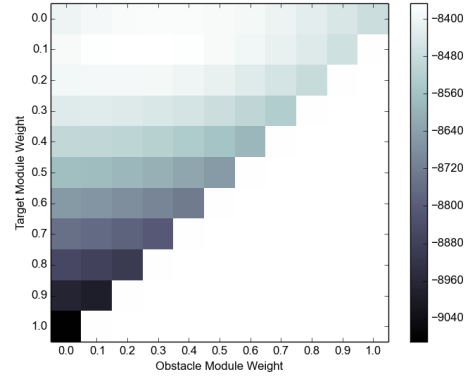
## 5 Conclusions

We analyzed human behavior using inverse modular reinforcement learning. The experimental results show that modular reinforcement learning can explain human behavior well, even though the performance of the agent is currently inferior to human subjects'.

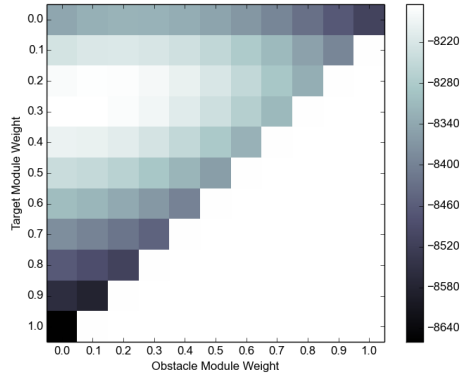
Note that a weighted sum of Q functions is just one way to combine multiple sub-MDPs. Other ways are possible, including, for example, scheduling between different modules, with only one active at one time. This is also called *skill* in the literature [2]. However, we adopt the weighted sum approach because this is more reasonable for human behavior. When a human tries to collect targets while avoiding obstacles, these two modules are expected to be both active. A scheduling approach may yield frequent oscillation between these two modules. Note also that we assume independence between modules. However, correlation between modules doesn't impair our analysis in this paper. In Figure 4, we can tell that the target module and obstacle module tend to be negatively correlated from the shape of the white zones. Lastly, weights may be dynamic and different from state to state. However, with such an assumption we need to learn a mapping from state to weights. In this case, the curse of dimensionality still exists, and inverse learning would be difficult.



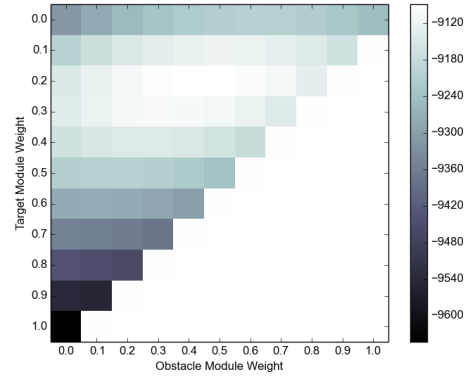
(a) Path following only.



(b) Obstacle + Path.



(c) Target + Path.



(d) Target + Obstacle + Path.

Figure 4: Heatmaps of the log of the values of Equation 1 for different weights for the four tasks, respectively. The white zones indicate higher probabilities. The weights of all three modules sum to 1, so we only show the weights on the target and the obstacle modules.

## References

- [1] Thomas G Dietterich. Hierarchical reinforcement learning with the maxq value function decomposition. *J. Artif. Intell. Res.(JAIR)*, 13:227–303, 2000.
- [2] George Konidaris and Andre S Barreto. Skill discovery in continuous reinforcement learning domains using skill chaining. In *Advances in Neural Information Processing Systems*, pages 1015–1023, 2009.
- [3] Andrew Y Ng, Stuart J Russell, et al. Algorithms for inverse reinforcement learning. In *Icml*, pages 663–670, 2000.
- [4] Constantin A Rothkopf. Inferring human intrinsic rewards through inverse reinforcement learning. *Frontiers in Computational Neuroscience*, (50), 2013.
- [5] Constantin A Rothkopf and Dana H Ballard. Modular inverse reinforcement learning for visuomotor behavior. *Biological cybernetics*, 107(4):477–490, 2013.
- [6] Nathan Sprague and Dana Ballard. Multiple-goal reinforcement learning with modular sarsa (0). In *IJCAI*, pages 1445–1447. Citeseer, 2003.
- [7] Nathan Sprague, Dana Ballard, and Al Robinson. Modeling embodied visual behaviors. *ACM Transactions on Applied Perception (TAP)*, 4(2):11, 2007.
- [8] Richard S Sutton and Andrew G Barto. *Reinforcement learning: An introduction*, volume 1. Cambridge Univ Press, 1998.
- [9] M. H. Tong and M. M. Hayhoe. Modeling uncertainty and intrinsic reward in a virtual walking task. *Journal of Vision*, 14(10):5, August 2014.